The EMBO Journal Vol.18 No.11 pp.3119–3132, 1999

Mechanism of non-spliceosomal mRNA splicing in the unfolded protein response pathway

Tania N.Gonzalez, Carmela Sidrauski, Silke Dörfler and Peter Walter[1]

Howard Hughes Medical Institute and Department of Biochemistry and Biophysics, University of California at San Francisco, San Francisco, CA 94143-0448, USA

[1]Corresponding author
e-mail: walter@cgl.ucsf.edu

The unfolded protein response is an intracellular signaling pathway that, in response to accumulation of misfolded proteins in the lumen of the endoplasmic reticulum (ER), upregulates transcription of ER resident chaperones. A key step in this pathway is the non-conventional, regulated splicing of the mRNA encoding the positive transcriptional regulator Hac1p. In the yeast *Saccharomyces cerevisiae*, the bifunctional transmembrane kinase/endoribonuclease Ire1p cleaves *HAC1* mRNA at both splice junctions and tRNA ligase joins the two exons together. We have reconstituted *HAC1* mRNA splicing in an efficient *in vitro* reaction and show that, in many ways, the mechanism of *HAC1* mRNA splicing resembles that of pre-tRNA splicing. In particular, Ire1p endonucleolytic cleavage leaves 2′,3′-cyclic phosphates, the excised exons remain associated by base pairing, and exon ligation by tRNA ligase follows the same chemical steps as for pre-tRNA splicing. To date, this mechanism of RNA processing is unprecedented for a messenger RNA. In contrast to the striking similarities to tRNA splicing, the structural features of the splice junctions recognized by Ire1p differ from those recognized by tRNA endonuclease. We show that small stem–loop structures predicted to form at both splice junctions of *HAC1* mRNA are required and sufficient for Ire1p cleavage.

Keywords: endoplasmic reticulum/Ire1p/mRNA splicing/tRNA ligase/unfolded protein response

Introduction

The lumen of the endoplasmic reticulum (ER) is a highly specialized compartment in eukaryotic cells. Secretory and most membrane proteins are folded, covalently modified and oligomerized in this compartment with the assistance of specialized ER resident proteins (Gething and Sambrook, 1992). It is only after proper folding and oligomeric assembly that proteins are able to continue their journey through the secretory pathway to the cell surface or to ER-distal compartments, such as the Golgi apparatus or lysosomes (Hammond and Helenius, 1995). Perturbations in the ER lumenal environment can thus be highly detrimental, as they can block production of many essential cellular components. Regulatory networks have evolved to detect and respond to changes in the ER, thus enabling cells to maintain an optimal folding environment in the ER. An example of this is the unfolded protein response (UPR), an ER to nucleus signaling pathway found in all eukaryotic cells, which is induced by accumulation of unfolded proteins in the ER. The UPR enables cells to increase the folding capacity of the ER lumen by increasing the transcription of genes encoding ER resident proteins that mediate protein folding, such as BiP, an hsp70-like chaperone, or PDI, an enzyme that catalyzes disulfide bond formation (reviewed in Shamu *et al*., 1994; Chapman *et al*., 1998; Sidrauski *et al*., 1998).

Four factors involved in UPR signaling have been identified in the yeast *Saccharomyces cerevisiae*: Ire1p, a transmembrane serine/threonine kinase that also exhibits site-specific endoribonuclease activity (Cox *et al*., 1993; Mori *et al*., 1993; Sidrauski and Walter, 1997); Ptc2p, a serine/threonine phosphatase thought to modulate the activity of Ire1p (Welihinda *et al*., 1998); tRNA ligase, an RNA processing enzyme required for splicing of tRNA precursors (Greer *et al*., 1983; Phizicky *et al*., 1992; Sidrauski *et al*., 1996; Sidrauski and Walter, 1997); and Hac1p, a member of the leucine zipper family of transcription factors (Cox and Walter, 1996; Mori *et al*., 1996; Nikawa *et al*., 1996).

Ire1p is localized to the ER and/or inner nuclear membranes, which are contiguous with one another. The N-terminal half of Ire1p lies in the ER lumen (Mori *et al*., 1993), where it senses by an unknown mechanism increases in the concentration of misfolded proteins. The kinase and endoribonuclease domains of Ire1p map to its C-terminal half and are located in either the cytoplasm or nucleus, where they induce downstream events in the UPR pathway. Like many other transmembrane kinases, oligomerization of Ire1p in the plane of the membrane induces its kinase activity and leads to Ire1p phosphorylation (Shamu and Walter, 1996; Welihinda and Kaufman, 1996). Concomitantly, the Ire1p endoribonucleolytic activity is induced (Sidrauski and Walter, 1997). The only substrate of Ire1p endoribonuclease known to date is the mRNA encoding the UPR-specific transcription factor Hac1p.

Hac1p upregulates transcription of genes encoding ER resident proteins by binding to a common regulatory sequence in their promoters, the UPR element (UPRE) (Mori *et al*., 1992, 1996; Kohno *et al*., 1993; Cox and Walter, 1996; Nikawa *et al*., 1996). Interestingly, Hac1p is regulated by changes in its abundance (Cox and Walter, 1996; Kawahara *et al*., 1997); the level of Hac1p, in turn, is controlled by the regulated splicing of its mRNA. In the absence of splicing, *HAC1* mRNA translation is inhibited due to the presence of a 252 nucleotide intron (Chapman and Walter, 1997; Kawahara *et al*., 1997). The mechanism by which the presence of the intron attenuates translation of *HAC1* mRNA is currently unknown.

Removal of the intron occurs by a non-conventional reaction mechanism that is catalyzed by Ire1p and tRNA ligase (Sidrauski and Walter, 1997). Upon accumulation of unfolded proteins in the ER, Ire1p initiates splicing by cleaving *HAC1*^{u} mRNA (*u* for *uninduced*) to liberate the intron, and the 5′ and 3′ exons. The two exons are subsequently joined by tRNA ligase to produce *HAC1*^{i} mRNA (*i* for *induced*), which is efficiently translated to produce Hac1p. Thus, the regulated splicing of *HAC1* mRNA is a key regulatory step in the UPR signaling pathway.

Although best understood in yeast, the salient features of this unusual signaling pathway are likely to be conserved in all eukaryotic cells. Homologues of Ire1p have been identified in *Caenorhabditis elegans* and in mammalian cells. The mammalian homologues are likely to function in a corresponding UPR pathway as is suggested from the phenotype of dominant negative mutants in these components (Tirasophon *et al*., 1998; Wang *et al*., 1998). Moreover, we have recently shown that mammalian cells accurately splice the yeast *HAC1* mRNA intron (M.Niwa and P.Walter, unpublished results). Thus, both the signal transduction components and mechanism appear phylogenetically conserved from yeast to mammals. This conservation makes it likely that our understanding of the molecular mechanism of the UPR in yeast will be directly applicable to our understanding of the corresponding pathway in human cells, where defects in protein folding in the ER can lead to devastating diseases (Kuznetsov and Nigam, 1998).

The splicing of *HAC1* mRNA by Ire1p and tRNA ligase is unprecedented, and little is known regarding its mechanism. Significantly, tRNA ligase, an enzyme previously thought to function exclusively in the splicing of pre-tRNAs, has been shown both *in vivo* and *in vitro* to participate in this reaction (Sidrauski *et al*., 1996; Sidrauski and Walter, 1997). In fact, we have previously shown that Ire1p and tRNA ligase are sufficient to splice *HAC1*^{u} mRNA *in vitro*, supporting the notion that these are the only two components absolutely required for the reaction. This is in striking contrast to splicing of all other pre-mRNAs which require >100 proteins and small nuclear RNAs constituting the spliceosome and its associated components (Moore *et al*., 1993). Pre-tRNA splicing, on the other hand, is more akin to *HAC1* mRNA splicing in that it also requires only two components for cleavage and ligation, tRNA endonuclease and tRNA ligase (Greer *et al*., 1983; Peebles *et al*., 1983; Belford *et al*., 1993). Thus, we previously speculated that pre-tRNA and *HAC1*^{u} mRNA splicing occur by similar mechanisms.

The mechanism by which pre-tRNAs are spliced is well understood (reviewed in Westaway and Abelson, 1995; Abelson *et al*., 1998). tRNA endonuclease cleaves precursor tRNA, releasing base-paired 5′ and 3′ exons and a linear intron. Cleavage generates a 2′,3′-cyclic phosphate terminus at the 3′ end of the 5′ exon, and a 5′-OH terminus at the 5′ end of the 3′ exon (Knapp *et al*., 1979; Peebles *et al*., 1983). The two exons are subsequently joined in a series of reactions catalyzed by the multifunctional enzyme tRNA ligase (Greer *et al*., 1983; Xu *et al*., 1990; Belford *et al*., 1993). The first step involves opening of the terminal 2′,3′-cyclic phosphate to leave a 2′-phosphate at the 3′ end of the 5′ exon. The 3′ exon is phosphorylated at its 5′ terminus after transfer of γ-phosphate from either GTP or ATP. Thus, the phosphate group derived from the γ-position of a nucleotide triphosphate ultimately links the two exons in the spliced mRNA. The 5′ terminal phosphate is next activated by the transfer of AMP from tRNA ligase to form a high energy 5′–5′ phosphoanhydride bond. Ligation occurs with the concomitant release of the AMP activating group. The 2′ phosphate remaining at the splice junction is later removed from spliced tRNA by a third enzyme, nicotinamide adenine dinucleotide (NAD)-dependent 2′-phosphotransferase (McCraith and Phizicky, 1990; Spinelli *et al*., 1997).

By extension, processing of *HAC1*^{u} mRNA may proceed in a manner similar to that outlined above. Indeed, both reactions are initiated by highly substrate-specific endoribonucleases (Peebles *et al*., 1983; Di Nicola Negri *et al*., 1997; Sidrauski and Walter, 1997). In addition, both endonucleases cleave their substrate 5′ and 3′ splice junctions independently of one another and in no obligate order (Miao and Abelson, 1993; Sidrauski and Walter, 1997; Kawahara *et al*., 1998). Therefore, they share a splicing chemistry that is strictly incompatible with the spliceosome-catalyzed mechanism, where cleavage of the 3′ splice junction must always follow the cleavage of the 5′ splice junction (Moore *et al*., 1993). However, Ire1p and tRNA endonuclease lack any significant similarity in amino acid sequence or subunit composition. Whereas tRNA endonuclease is a tetramer composed of four different polypeptide chains (Trotta *et al*., 1997) that constitutively splices precursor tRNA, Ire1p is composed of one subunit that is thought to homo-oligomerize (Shamu and Walter, 1996; Welihinda and Kaufman, 1996) and its endoribonucleolytic activity is tightly regulated by conditions in the ER lumen. Furthermore, Ire1p and tRNA endonuclease differ significantly with respect to their substrate recognition. tRNA endonuclease recognizes the folded tertiary structure of pre-tRNA, as well as local structures at the intron–exon boundaries, and pays little attention to the sequence at or near the splice sites (Mattoccia *et al*., 1988; Reyes and Abelson, 1988; Fabbri *et al*., 1998). In contrast, point mutations generated near the splice junctions of *HAC1* mRNA have been shown to block its splicing both *in vivo* and *in vitro* (Sidrauski and Walter, 1997; Kawahara *et al*., 1998). To address questions regarding both the similarities and differences in the mechanism of *HAC1* mRNA and pre-tRNA splicing experimentally, we have developed efficient *in vitro* reactions which have allowed us to characterize the mechanism and the substrate requirements for *HAC1* mRNA splicing.

Results

The predicted HAC1 mRNA splice junction stem–loops act as Ire1p minisubstrates

As previously shown, Ire1p is a site-specific endoribonuclease that cleaves *HAC1*^{u} mRNA at both splice junctions (Sidrauski and Walter, 1997). Cleavage at either junction can occur independently of cleavage at the other junction; cleavage specificity, therefore, must result from either sequence and/or structural motifs that are common to both splice junctions. Indeed, the predicted secondary structure of the *HAC1*^{u} intron (Figure 1) reveals similar stem–loop

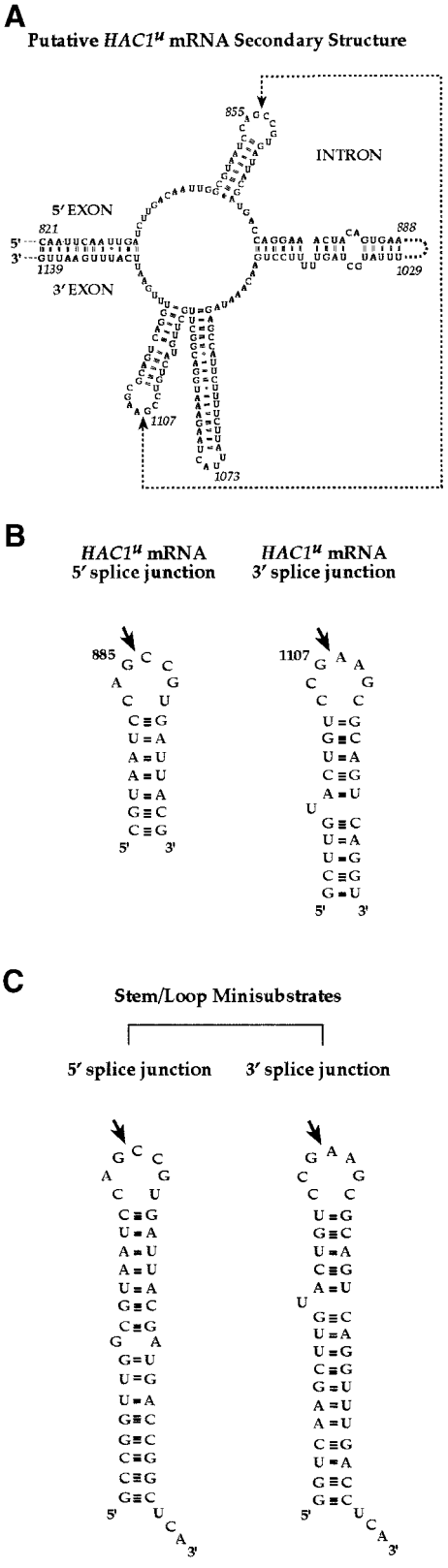

Fig. 1. Secondary structure prediction of the *HAC1*^{u} mRNA intron and splice site stem–loop structures. The secondary structure prediction of the *HAC1*^{u} mRNA intron and flanking 5′ and 3′ exon regions is shown (**A**) together with a close-up view of predicted stem–loop structures at the 5′ and 3′ splice sites (**B**). Ire1p(k+t) cleavage sites are indicated by arrows and were confirmed in Figure 6. (**C**) Sequence and predicted structures of the minisubstrate stem–loop RNAs used in this study.

structures at the 5′ and 3′ splice site junctions (Sidrauski and Walter, 1997; Kawahara *et al*., 1998). At either site, the RNA is predicted to fold into short stems with 7-nucleotide loops, each containing a G residue in the third position. Previous work suggested that nucleolytic cleavage by Ire1p occurs at this invariant G, but conflicting models have been proposed as to whether Ire1p cleaves at its 5′ or 3′ side (Kawahara *et al*., 1997; Sidrauski and Walter, 1997).

To analyze the substrate specificity and the chemistry of the Ire1p-mediated cleavage reaction, we first asked whether the stem–loop structure that is proposed in Figure 1B would be sufficient to direct Ire1p cleavage. To this end, we designed 'minisubstrates', two short RNA molecules shown in Figure 1C that are predicted to fold into structures similar to those predicted at either splice site for authentic *HAC1*^{u} mRNA. In these minisubstrate stem–loop RNAs, we extended the lengths of the stems by five or six base pairs with unrelated sequences to stabilize the stems. A 3-nucleotide 3′ extension was also added so that the anticipated cleavage products could be more easily distinguished by their size. Stem–loop RNAs were made by *in vitro* transcription with T7 polymerase using synthetic DNA oligonucleotide templates. Transcripts were uniformly labeled during transcription by incorporation of [^{32}P]UTP and gel purified.

When incubated with a fragment of Ire1p termed Ire1p(k+t) (Sidrauski and Walter, 1997), which contains the Ire1p kinase domain and C-terminal tail domain and which has been proposed to contain the nuclease active site, the stem–loop RNAs corresponding to either splice site were efficiently cleaved to produce two discrete fragments (Figure 2A). The size of the cleavage products suggested that cleavage occurred at or in close proximity to the predicted site. Cleavage of RNA that was either internally labeled with [α-^{32}P]UTP during transcription (Figure 2B, lane 4), or that was transcribed in the absence of labeled nucleotide and then labeled at the 5′ terminus with [γ-^{32}P]ATP and polynucleotide kinase (Figure 2B, lane 3), confirmed that the faster migrating band corresponded to the 5′ end of the RNA.

To ascertain that the stem–loop RNAs behaved similarly to authentic *HAC1*^{u} RNA, we tested the ability of Ire1p(k+t) to cleave our minisubstrates carrying single nucleotide substitutions in loop residues. Previous studies had identified mutations in the predicted loops that prevent Ire1p from cleaving *HAC1*^{u} mRNA *in vitro* or *in vivo*. Indeed, as shown in Figure 2B (lane 6), a G→C mutation in the loop corresponding to position 1107 in the full-length *HAC1*^{u} mRNA completely abolished cleavage of the 3′ stem–loop RNA as previously shown for authentic *HAC1*^{u} mRNA (Sidrauski and Walter, 1997). Likewise, mutations at two other loop positions (C1105G and G1110C), each representing additional invariant bases found at both splice sites, also prevented cleavage by Ire1p(k+t) (Figure 2B, lanes 5 and 7), consistent with previous *in vivo* splicing data (Kawahara *et al*., 1998). Thus all three residues in the loop whose positions are invariant between both splice junctions are critical for Ire1p(k+t) cleavage.

To obtain a complete picture of the constraints that loop residues put on the Ire1p(k+t) cleavage reaction, we tested a series of mutant 3′ stem–loop minisubstrates in which

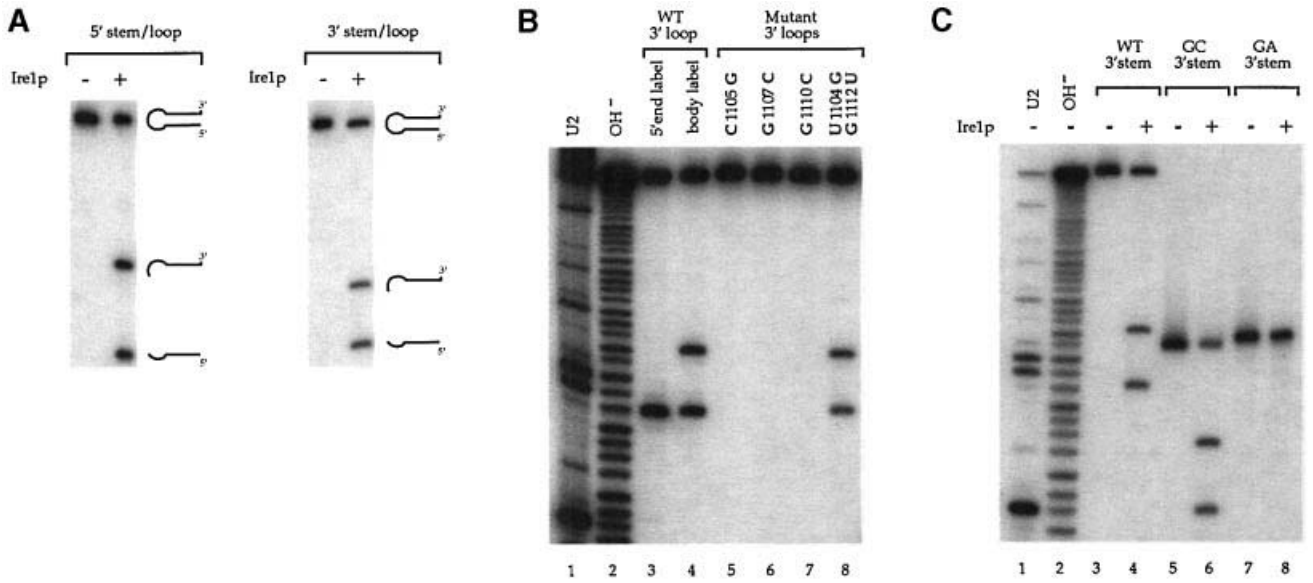

Fig. 2. Cleavage of stem–loop RNAs by Ire1p(k+t). (**A**) Radiolabeled *in vitro* transcribed 5′ stem–loop RNA (2000 c.p.m.) (lanes 1 and 2) and 3′ stem–loop RNA (2000 c.p.m.) (lanes 3 and 4) as shown in Figure 1C, were incubated in cleavage buffer (see Materials and methods) in the presence or absence of 1 µg Ire1p(k+t) at 30°C for 2 h. The reaction volume was 20 µl. The reaction products were separated on denaturing polyacrylamide gel and visualized by autoradiography. (**B**) The results of incubation of various mutant loop RNAs with Ire1p(k+t) are shown in lanes 5–8, with the specific loop mutation given above each lane. Refer to Figure 1 to place these in the context of the wild-type 3′ stem–loop. Lanes 1 and 2 carry markers produced by nuclease U2 digestion (lane 1) or alkaline hydrolysis (lane 2) of 5′ end-labeled wild-type 3′ stem–loop RNA. Lanes 3 and 4 contain 5′ end-labeled (lane 3) and internally labeled (lane 4) wild-type 3′ stem–loop RNAs that were cleaved with Ire1p(k+t), respectively. (**C**) The following RNAs were incubated in the presence or absence of Ire1p(k+t) as indicated: wild-type 3′ stem–loop RNA (lanes 3 and 4), a 3′ stem–loop RNA in which the wild-type stem sequence was replaced by a stem of GC base pairs (see Materials and methods) (lanes 5 and 6), and a 3′ stem–loop where every C of the GC stem was replaced by an A (lanes 7 and 8) to abolish base pairing. Note that the substrates in lanes 5–8 are 10 nucleotides shorter than the wild-type 3′ stem–loop RNA in lanes 3 and 4. Lanes 1 and 2 are as in (B).

each loop nucleotide was individually changed to every other ribonucleotide. These data, summarized in Figure 3, show that there is a hierarchy of importance. Most notably, no base substitution was tolerated at the three invariant bases (C1105, G1107 and G1110) that are common to both splice sites. As indicated in Figure 3, these residues are located at positions –3, –1 and +3 with respect to the splice site. Loop position +1 could only be an A or a C, which corresponds to the bases found at the 3′ and 5′ splice junction. Both A and C provide an H-bond donor (a primary amine) as well as an H-bond acceptor (a tertiary amine) at the same position on the 6-membered ring of each nucleotide. This may indicate a role for these functional groups for structuring the loop and/or for forming contacts with Ire1p(k+t). In position –2 all four bases worked equally well, whereas the other two positions (+2 and +4) showed some, albeit weak preference for the bases found at the wild-type 3′ splice site. Interestingly, mutating these residues to those found at the 5′ splice junction reduced cleavage, suggesting that these positions may be sensitive to the sequence context present in either loop. Overall, the effects of these mutations on Ire1p(k+t) cleavage could reflect sequence-specific and/or structural constraints required for Ire1p(k+t) recognition of these minisubstrates.

Mutations predicted to allow pairing of the bases at positions –3, +4 (C–3 to G, or C+4 to G), and hence predicted to create a smaller 5-base loop, abolished cleavage. Likewise, a mutation changing U at position –4 to an A and hence predicted to open the ultimate base pair of the stem impaired cleavage. Taken together, these results suggest that the loop must be constrained to its wild-type length of 7 nucleotides to fold into a defined tertiary structure. Additional support for folding of the bases into a structured loop was obtained by S1 nuclease probing experiments. S1 nuclease cleaves single-stranded RNA without regard to primary sequence. Only the bonds following the nucleotides at the –1 and +1 positions were sensitive to S1 nuclease cleavage (data not shown), suggesting that the remaining 5-loop residues are inaccessible to the S1 nuclease.

With the exception of positions +1 and –4, our results are consistent with data from a previous study investigating *HAC1* mRNA splicing *in vivo*. In this study, changing position +1 from A to U or changing position –4 from U to A reduced splicing by 25% or less (Kawahara *et al*., 1998). This discrepancy most likely reflects the fact that Ire1p interactions with *HAC1*^{u} mRNA are stronger than those with the stem–loop minisubstrates.

We next confirmed the importance of the stem for Ire1p(k+t) cleavage. Switching the bases that form the proposed U–G pair closing the loop did not diminish cleavage (Figure 2B, lane 8), suggesting that the nucleotide sequence is not important as long as the regions flanking the 7-membered loop can form a stable stem. To test this notion further, we made a stem–loop in which all base pairs in the stem, with the exception of the UG pair that closes off the loop, were changed to GC or CG pairs. Due to the high melting temperature of GC and CG base pairs, we were also able to shorten the stem down to 11 bp from the 16 bp used in our original 3′ stem–loop minisubstrate (Figure 1C). Ten base pairs is the predicted length of the 3′ stem–loop within the intact *HAC1*^{u} mRNA (Figure 1A and B). As shown in Figure 2C, lanes 5 and 6, cleavage

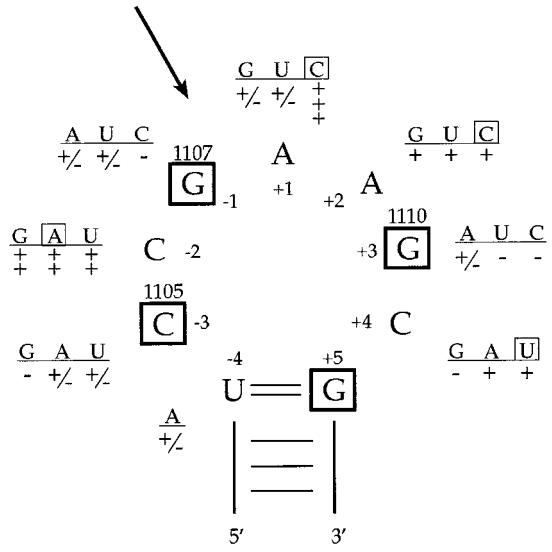

Fig. 3. Mutational analysis of 3′ splice site loop. A series of twenty-two 3′ stem–loop mutants, each carrying a single loop point mutation, was transcribed and radiolabeled as in Figure 2. The wild-type 3′ loop sequence is shown with the 4 nucleotides whose positions are invariant between 5′ and 3′ splice junction stem–loops boxed in bold and their nucleotide position indicated above (refer to Figure 1A and B). In addition, each loop residue has been assigned a (+) or (–) number relative to the Ire1p(k+t) cleavage site indicated by an arrow. The sequence of the various point mutants is indicated next to each loop residue. Of these, those which are boxed indicate the equivalent residue at that position in the 5′ loop (refer to Figure 1). Indicated below these sequences is the extent to which each was cleaved by Ire1p(k+t). Values are reported as the fraction (mutant cleavage/wild-type cleavage) where: (–) no cleavage; (+/–) 0–10%; (+) 10–60%; (++) 60–120%; (+++) ⩾120%. Ire1p(k+t) reactions were performed as described in Figure 2.

occurred at about the same level as found for stem–loops with the authentic *HAC1*^{u} mRNA sequence (lanes 3 and 4). We next changed all Cs of the stem to As. This drastic change, predicted to disrupt the stem completely, abolished cleavage (Figure 2C, lanes 7 and 8). Thus we conclude that an intact stem is important, but that, in contrast to the loop, the nucleotide sequence of the residues that form the stem is irrelevant for cleavage by Ire1p(k+t). Taken together, these results show that the stem–loop minisubstrates represent the minimal RNA element that is required and sufficient for Ire1p(k+t) cleavage.

Ire1p(k+t) cleavage generates 2′,3′-cyclic phosphodiester termini

Having confirmed that Ire1p(k+t) processes our minisubstrates with specificity indistinguishable from *HAC1*^{u} mRNA, we used these simplified substrates to explore the chemistry of the Ire1p(k+t) cleavage reaction. To this end, we employed nearest neighbor analysis to determine the nature of the RNA termini produced upon Ire1p(k+t) cleavage. Stem–loop RNAs corresponding to either the 5′ (Figure 4A) or 3′ splice junction (Figure 4B) were labeled by incorporation of [α-^{32}P]CTP, [α-^{32}P]GTP or [α-^{32}P]ATP as indicated above the lanes. Digestion of the transcription products with P1 nuclease (which cleaves RNA to leave 5′-phosphate and 3′-OH groups) generated the expected 5′-monophosphorylated nucleotides as shown by thin layer chromatography (TLC) (Figure 4A and B, lanes 1–3), confirming that the labeled stem–loop RNAs contained labeled phosphate groups only in the appropriate positions.

In contrast, a new labeled nucleotide species was observed on thin layer plates when the transcription products were first cleaved with Ire1p(k+t) and the isolated 5′ fragment was then digested with P1 nuclease (‘pG>p’, Figure 4A and B, lanes 4–6). This spot comigrated with synthetic 5′-phosphate-guanosine-2′,3′-cyclic phosphate (here abbreviated pG>p), indicating that Ire1p(k+t) cleaves RNA to leave a 2′,3′-phosphate (note that nuclease P1 does not cleave at 2′,3′-cyclic phosphate groups). Consistent with this notion, labeled pG>p was only observed when the 5′ stem–loop RNA was labeled with [α-^{32}P]GTP (producing [^{32}P]G>p) or [α-^{32}P]CTP (producing pG>[^{32}P]) (Figure 4A, lanes 4 and 5), or when the 3′ stem–loop RNA was labeled with [α-^{32}P]GTP or [α-^{32}P]ATP (Figure 4B, lanes 5 and 6). Thus we conclude that Ire1p(k+t) cleaves the stem–loop RNAs at the 3′ side of the invariant G found in the third position of the loop. Furthermore, unlike any other mRNA splicing intermediate, Ire1p(k+t) produces a 2′,3′-cyclic phosphate group at its cleavage site. The reaction is more reminiscent of that of tRNA endonuclease which cleaves pre-tRNAs to produce 2′,3′-cyclic phosphate termini (Peebles *et al*., 1983).

Since there is no precedent for an mRNA splicing intermediate with 2′,3′-cyclic phosphate termini, we decided to confirm our observations by using a series of sequential enzymatic modifications to simultaneously analyze the termini of the 3′ and 5′ cleavage fragments. We took advantage of the fact that the fragments produced upon Ire1p(k+t) cleavage of the stem–loop RNAs were small enough so that charge differences due to the presence or absence of terminal phosphate groups altered their electrophoretic mobilities in polyacrylamide gels. As shown in the diagram in Figure 5A, we first used calf intestinal phosphatase (CIP) to remove non-cyclic terminal phosphates. This resulted in a decreased mobility of the 5′ fragment, consistent with the predicted loss of its 5′-triphosphate group, and no mobility change in the 3′ fragment (Figure 5B, lane 2). Next, we treated the fragments produced thus with T4 polynucleotide kinase (T4 PNK) which hydrolyzes 2′,3′-cyclic terminal phosphates. Loss of the additional phosphate group led to a further reduction of the mobility of the 5′ fragment (Figure 5B, lane 3). This provided independent confirmation of the results presented in Figure 4, by demonstrating that a cyclic phosphate was produced at the 3′ end of the 5′ fragment, since a non-cyclic phosphate would have already been removed by CIP in the preceding step. Finally, we used treatment with T4 PNK in the presence of ATP to phosphorylate free 5′-OH groups. This led to an increased mobility of both the 5′ and 3′ fragment (Figure 5B, lane 4), indicating that the Ire1p(k+t)-produced 3′ fragment terminates in a 5′-OH group that can be phosphorylated.

The assignment of the Ire1p(k+t) cleavage site on the 3′ side of the invariant G in the loop was in conflict with an earlier study from our laboratory. In particular, primer extension mapped the Ire1p cleavage sites of *HAC1*^{u} mRNA to the 5′ side of the invariant G (Sidrauski and Walter, 1997). This raised the possibility that cleavage of the minisubstrates and that of authentic *HAC1*^{u} mRNA

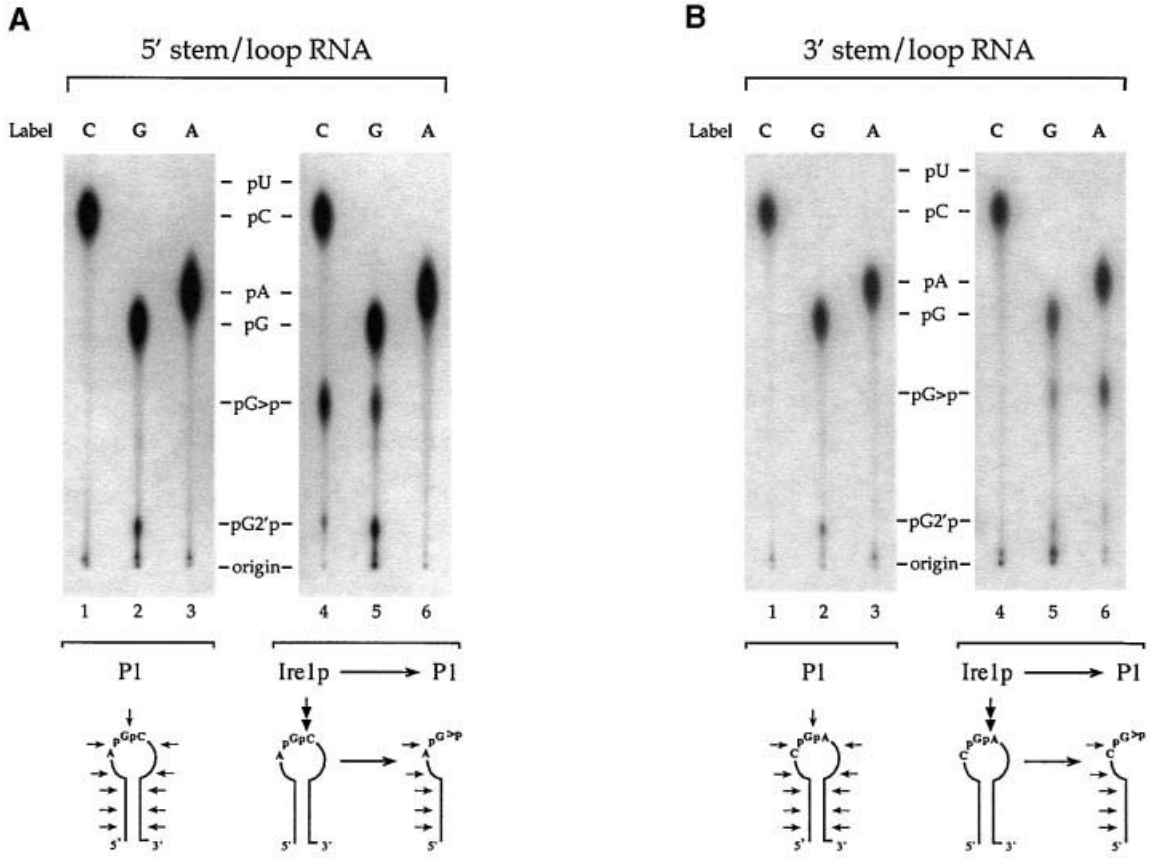

Fig. 4. Formation of 3′ terminal guanosine 2′,3′-cyclic phosphate after Ire1p(k+t) cleavage of stem–loop RNA. 5′ stem–loop RNA (**A**) or 3′ stem–loop RNA (**B**) was labeled with [α-^{32}P]CTP (lanes 1 and 4), [α-^{32}P]GTP (lanes 2 and 5) or [α-^{32}P]ATP (lanes 3 and 6). The labeled RNAs were then digested with P1 nuclease (lanes 1–3). Alternatively, they were first digested (40 000 to 60 000 c.p.m. of each stem–loop RNA) with Ire1p(k+t). The 5′ cleavage product was then isolated by preparative gel electrophoresis and digested with P1 nuclease (lanes 4–6). The final digestion products were separated by TLC on PEI cellulose plates and visualized by autoradiography. The position of marker nucleotides on the thin layer plates are indicated, where pG>p refers to a G bearing a 5′ phosphate and a 2′,3′-cyclic phosphate. Digestion of the relevant portions of the stem–loop structures is indicated schematically below each panel. The ratios of labeled pG>p relative to labeled pN were determined and are in good agreement with the expected values. (A) Lanes 4 and 5: pC/pG>p expected = 0.25, actual = 0.26; pG/pG>p expected =0.13, actual = 0.18. (B) Lanes 5 and 6: pG/pG>p expected = 0.17, actual = 0.21; pA/pG>p expected = 0.25, actual = 0.26. Note also that a variant of the wild-type 5′ stem–loop was used in this analysis (hactng-39). In this stem–loop, a GC dinucleotide pair in the stem was changed, leaving the only GC dinucleotide in the loop. The only GA dinucleotide in the wild-type 3′ stem–loop (hactng-10) was in the loop.

might, in fact, be different. The previous studies, however, used oligonucleotide primers distant from the cleavage site, making it possible that the cleavage sites were misassigned. To address this discrepancy and to verify that the cleavage sites in the minisubstrates and intact *HAC1^u* mRNA were, in fact, identical, we repeated primer extension analysis on Ire1p(k+t)-cleaved *HAC1^u* 508 RNA (the same construct used previously) but using primers located closer to the cleavage sites (Figure 6). The analysis shows unambiguously that Ire1p(k+t) cleaves the 5′ and 3′ splice junctions of *HAC1^u* RNA at the 3′ side of the invariant Gs. These are the same positions at which Ire1p(k+t) cleaves the 5′ and 3′ stem–loop RNAs, thereby affirming the use of the minisubstrates to characterize the mechanism of the Ire1p(k+t)-catalyzed cleavage reaction.

Additional elements in HAC1^U mRNA contribute to Ire1p(k+t) cleavage efficiency

Although Ire1p(k+t) accurately cleaves the stem–loop substrates, additional structural and/or sequence elements present in *HAC1^u* RNA are likely to contribute significantly to the efficiency of the reaction. To compare the cleavage efficiencies of the different substrates, we analyzed time courses of *HAC1^u* RNA and stem–loop RNA Ire1p(k+t) digestions performed under identical conditions. Figure 7A shows a time course of *HAC1^u* RNA digestion. We note that the substrate RNA disappears rapidly with a half time of ~2 min (Figure 7A, filled diamonds). Digestion intermediates appear transiently in a manner reminiscent of classical pulse–chase kinetics (Figure 7A, open circles and open squares), and the liberation of 5′ and 3′ exons (crossed circles and crossed squares) occurs rapidly and at comparable rates. In contrast, liberation of the intron (open triangles) follows a short lag time, concordant with the fact that two sequential cleavage events are required for its production. Taken together, these kinetics are consistent with a reaction in which both splice sites are cleaved independently and in random order (Sidrauski and Walter, 1997; Kawahara *et al*., 1998).

In contrast, the smaller stem–loop RNAs were cleaved at significantly reduced rates. After 8 h of incubation under identical reaction conditions, <25% of either stem–loop RNA was cleaved (Figure 7B and C), whereas cleavage of *HAC1^u* RNA was virtually complete within 16 min. Incubation of both the 5′ and 3′ stem–loops

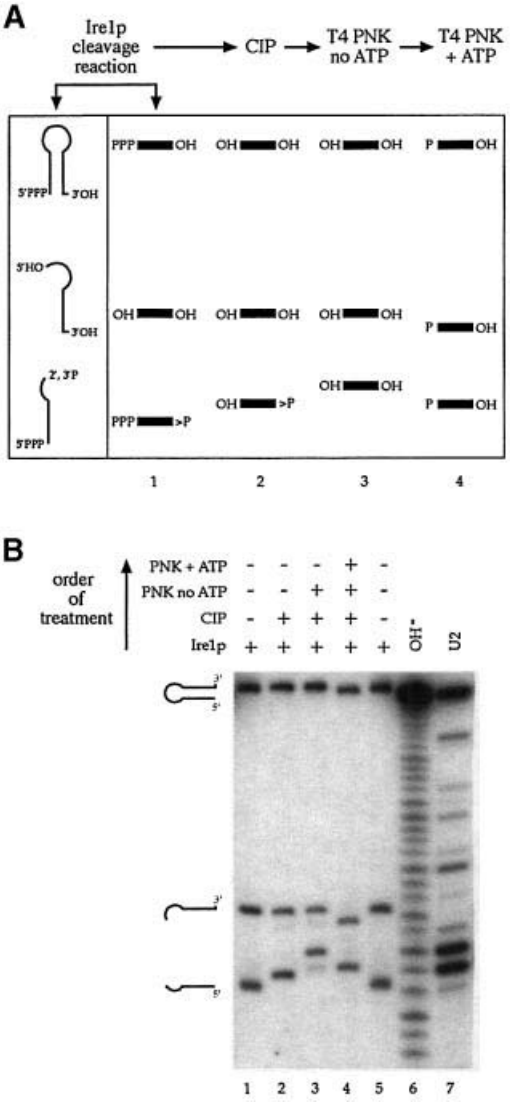

Fig. 5. Characterization of termini produced after Ire1p(k+t) cleavage of stem–loop RNA by sequential enzymatic modification. (**A**) A schematic of the cleavage products generated upon Ire1p(k+t) cleavage and subsequent enzymatic modification of stem–loop RNA is shown. Different gel mobilities of the short fragments result from charge differences due to terminal phosphate groups as indicated. '>P' represents a 2′,3′-cyclic phosphate. Lanes 1–4 correspond to lanes 1–4 in (B). (**B**) Ire1p(k+t) cleavage of internally labeled 3′ stem–loop RNA was performed as described in Figure 2. Lanes 1 and 5 show the products of an Ire1p(k+t) cleavage reactions of 3′ stem–loop RNA. The products were then treated sequentially with CIP (lane 2), with T4 PNK in the absence of ATP (lane 3), and with T4 PNK in the presence of ATP (lane 4). Markers were produced by alkaline hydrolysis (lane 6) or nuclease U2 digestion (lane 7) of 5′ end-labeled wild-type 3′ stem–loop RNA.

together in the same reaction did not stimulate the cleavage of either stem–loop, nor did heating and quick cooling of the stem–loop substrates prior to their addition to the reaction (data not shown). We therefore conclude that structural elements of *HAC1*^{u} RNA, in addition to the stem–loop structures characterized here, must contribute significantly to the efficiency of cleavage by Ire1p(k+t), possibly by enhancing substrate recognition by Ire1p(k+t).

Ire1p(k+t) liberates base paired exons

The predicted secondary structure of the *HAC1*^{u} RNA intron (Figure 1A) suggested that the exon sequences

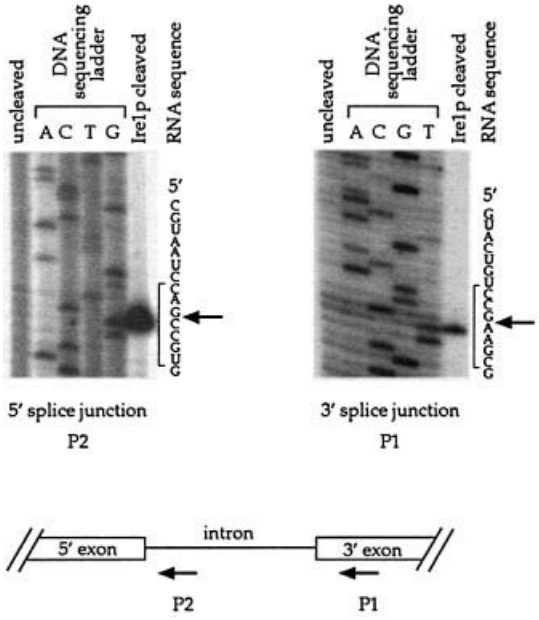

Fig. 6. Ire1p(k+t) cleaves *HAC1*^{u} RNA at the same positions as it cleaves the 5′ and 3′ stem–loops. Primer extension analysis was performed on both undigested and Ire1p(k+t)-digested *HAC1*^{u} 508 RNA using 5′ end-labeled DNA primers. *HAC1*^{u} 508 RNA consists of a truncated 5′ exon (181 nucleotides), an intact *HAC1*^{u} intron (252 nucleotides), and a truncated 3′ exon (75 nucleotides), as previously described (Sidrauski and Walter, 1997). Extensions on uncleaved RNA served as controls for natural pausing during the extension reaction. The Ire1p(k+t) cleavage site is indicated by an arrow along side the RNA sequence corresponding to the DNA ladder; the residues in the 7-membered loop are marked with a bracket.

flanking the intron are also base paired and hence may contribute to folding the intron–exon junctions into a more complex RNA domain. A prediction of the proposed structure is that the two exons remain associated after removal of the intron by Ire1p-mediated cleavage. To test this possibility directly, we fractionated Ire1p(k+t)-generated *HAC1*^{u} RNA cleavage products on a non-denaturing gel (Figure 8A). Individual bands were excised from the non-denaturing gel and re-electrophoresed under denaturing conditions to determine their composition (Figure 8B). Only two major bands were obtained when Ire1p(k+t)-digested *HAC1*^{u} RNA was fractionated under native conditions (Figure 8A, lane 1; labeled *a* and *b*). If the cleavage reaction products were first denatured by boiling, band *a* disappeared and two new, faster migrating bands appeared in its place (Figure 8A, lane 2; labeled *d* and *e*). As apparent from the analysis shown in Figure 8B, band *a* contains both exons which upon boiling become separated into band *d* containing the 5′ exon and band *e* containing the 3′ exon. Thus, upon Ire1p(k+t) digestion, the 5′ and 3′ exons remain non-covalently associated and comigrate in a native gel, whereas the intron is released. In the context of the *HAC1*^{u} RNA splicing reaction, this association may be advantageous in that it holds the two exons in position for efficient and specific ligation by tRNA ligase.

The phosphate linking the two exons of spliced HAC1 mRNA is derived from nucleotide triphosphate

The data presented so far show that, in many respects, the mechanism of *HAC1*^{u} mRNA splicing follows the

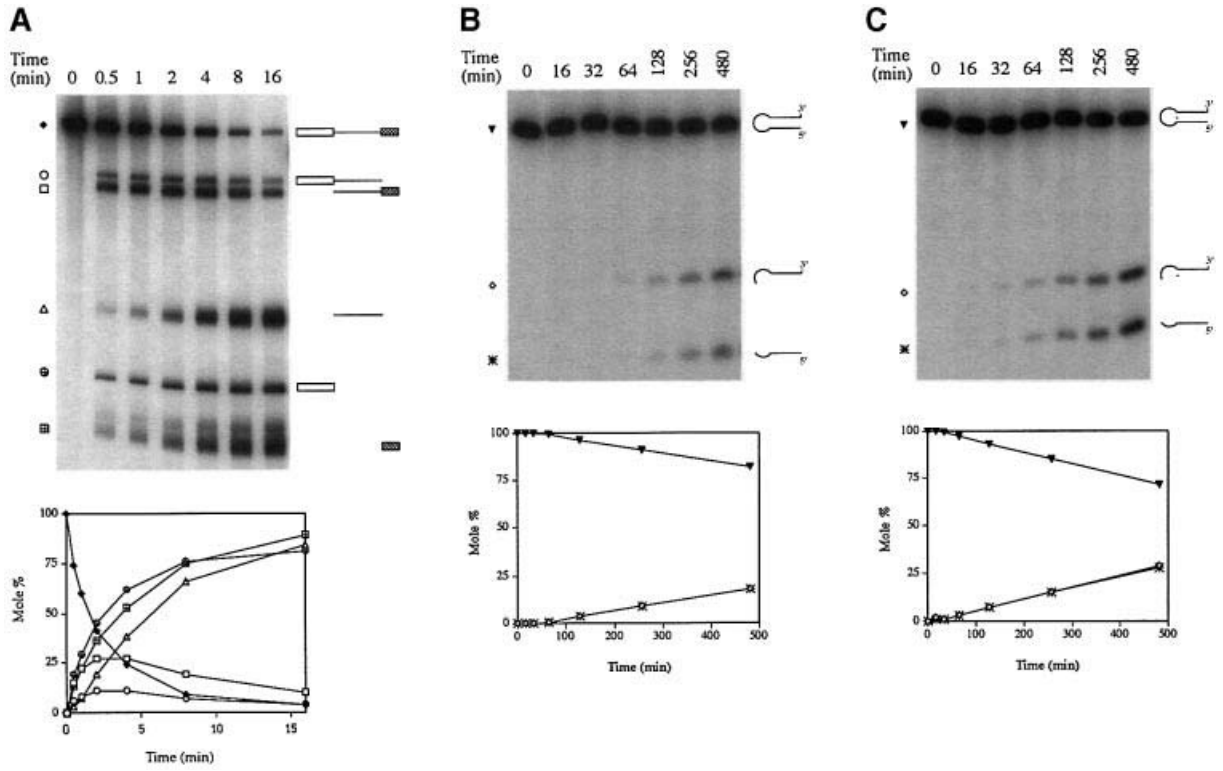

Fig. 7. Ire1p(k+t) cleaves *HAC1*^{u} RNA more efficiently than stem–loop RNAs. (**A**) A time course of *HAC1*^{u} 600 RNA cleavage is shown. *HAC1*^{u} 600 RNA consists of a truncated 5′ exon (181 nucleotides), an intact *HAC1*^{u} intron (252 nucleotides), and a truncated 3′ exon (167 nucleotides). A cocktail of 140 000 c.p.m. *HAC1*^{u} 600 RNA (0.07 pM), cleavage buffer, and 1.75 µg Ire1p(k+t) in a volume of 140 µl was incubated at 30°C. Samples (20 µl) were removed at the times indicated and the reactions were stopped by addition of 20 volumes phenol/chloroform and 20 volumes of stop buffer. Reactions were ethanol-precipitated, electrophoresed through a 5% denaturing polyacrylamide gel, visualized by autoradiography and quantitated. Percent conversion is the mole ratio (amount of fragment produced)/(amount of fragment expected if 100% cleavage occurred) adjusted for the number of labeled phosphate groups carried by each fragment. Symbols next to the autoradiogram correspond to the symbols used for each fragment in the graph below. The icons to the right represent the fragments produced in the Ire1p(k+t) cleavage reaction. A time course of 5′ stem–loop (**B**) and 3′ stem–loop RNA (**C**) cleavage is shown. Cocktails of 44 000 c.p.m. of stem–loop RNAs (0.22 pM), cleavage buffer and 5.5 µg Ire1p(k+t) in a volume of 440 µl were incubated at 30°C. Samples (40 µl) were removed at the times indicated, rapidly stopped and precipitated as described above, and electrophoresed through a 15% denaturing polyacrylamide gel. The mole ratio of Ire1p(k+t) to RNA substrate is identical in all panels. Visualization and quantitation as well as symbols and icons are as in (A). Note the significantly longer time scales of these experiments. Also note that the amount of Ire1p(k+t) used in the experiments shown in this figure was less than the amount used in the experiments shown in Figures 2 and 5 and thus accounts for the reduced cleavage of the stem–loop substrates at comparable time points.

paradigms established for pre-tRNA splicing (Westaway and Abelson, 1995; Abelson *et al*., 1998). During pre-tRNA splicing, tRNA ligase phosphorylates the 5′ end of the 3′ exon in a step prior to exon ligation. As a consequence, the phosphate group in the phosphodiester bond linking the 5′ and 3′ exons in spliced tRNAs originates from the γ-phosphate of the GTP or ATP used by tRNA ligase and not from the tRNA itself (Belford *et al*., 1993). To determine if this is also true for *HAC1*^{u} RNA splicing, we added purified tRNA ligase to Ire1p(k+t)-cleaved *HAC1*^{u} RNA, thus reconstituting a complete splicing *in vitro* reaction as previously described (Sidrauski and Walter, 1997). As shown in Figure 9A, ligation occurred very efficiently in our assay system; tRNA ligase addition to Ire1p(k+t)-cleaved *HAC1*^{u} RNA resulted in a virtually quantitative conversion of the exons (compare lanes 3 and 4) to the ligated product which comigrated with a marker transcript lacking the intron (Figure 8A, lane 1). This reaction was then repeated using unlabeled input RNA and [γ-^{32}P]GTP (Figure 9A, lane 5). Under these conditions, any incorporated radioactivity was exclusively derived from the γ-position of the added nucleotide triphosphate. Three prominent, labeled bands were obtained under these conditions (Figure 9A, lane 5), corresponding to the ligated exons, the intron and residual 3′ exon. Thus, as expected, tRNA ligase phosphorylated the two RNA fragments containing free 5′-OH groups (intron and 3′ exon), but not the 5′ exon as it already contains a 5′-triphosphate group. Importantly, these data also suggest that phosphorylated 3′ exon was incorporated into ligated RNA, as previously described for pre-tRNA splicing (Belford *et al*., 1993).

During pre-tRNA splicing, in the last step prior to exon ligation, tRNA ligase adenylates itself using ATP. Ligase then covalently transfers the AMP to the 5′ phosphate of the 3′ exon which results in the formation of a high energy 5′–5′ phosphoanhydride bond. Upon exon ligation, the AMP is released from the RNA (Greer *et al*., 1983; Xu *et al*., 1990). To determine if this is also true for *HAC1*^{u} RNA splicing, we incubated unlabeled input RNA with Ire1p(k+t), tRNA ligase and [α-^{32}P]ATP (Figure 9A, lanes 6 and 7). Under these conditions the 3′ exon and the intron were labeled. In addition, no label was incorporated into the fully spliced RNA. Both these

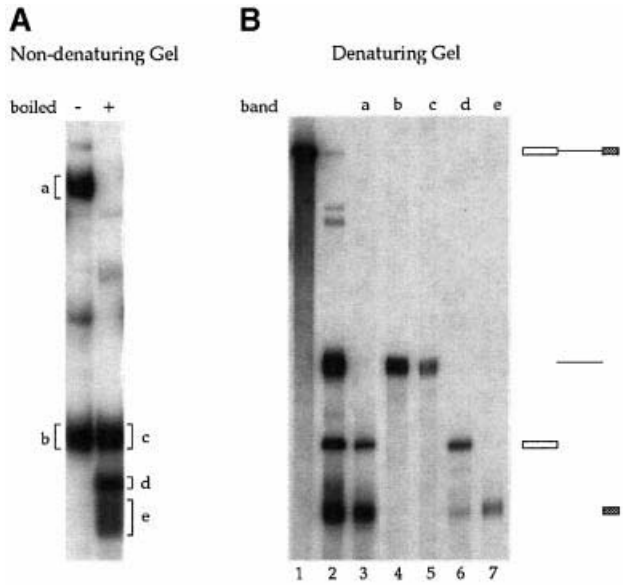

Fig. 8. *HAC1*^{u} RNA exons remain base paired following Ire1p(k+t) cleavage. (**A**) An aliquot of *HAC1*^{u} 600 RNA (40 000 c.p.m.) was incubated with 1 µg Ire1p(k+t) in cleavage buffer in 40 µl for 45 min at 30°C. As indicated, reactions were either boiled or not and electrophoresed under non-denaturing conditions through a 5% polyacrylamide gel in TBE and visualized by autoradiography. The bands labeled a, b, c, d and e were excised from the gel. The RNA was eluted from the gel slices overnight. (**B**) Eluted a, b, c, d and e RNAs were resuspended in denaturing loading buffer, boiled and electrophoresed through a 5% denaturing polyacrylamide gel. The marker lanes 1 and 2 carry uncleaved *HAC1*^{u} 600 RNA and Ire1p(k+t) cleaved *HAC1*^{u} RNA, respectively. Icons to the right of the figure indicate the fragments produced in the Ire1p(k+t) cleavage reaction.

observations suggest that *HAC1* exons are ligated by tRNA ligase utilizing the same mechanism with which tRNA exons are joined.

To show that the label in the spliced RNA was indeed incorporated at the splice junction, we took advantage of the fact that during pre-tRNA splicing, tRNA ligase opens up the 2′,3′-cyclic phosphate at the 3′ terminus of the 5′ exon and leaves this phosphate attached at the 2′ position of the splice junction. For our purposes, the presence of the 2′ phosphate would provide a convenient marker for the splice junction as it would render this single phosphodiester bond in the spliced RNA resistant to cleavage by P1 nuclease. To determine whether the labeled γ-phosphate group donated by GTP during the splicing reaction was indeed incorporated at the splice junction, we purified the spliced product from a reaction as shown in Figure 9A, lane 5, and subjected it to digestion with P1 nuclease. TLC of the digestion products revealed that the labeled phosphate was quantitatively recovered in a slow migrating spot (Figure 9B, lane 4) with a mobility identical to that of the marker nucleotide 5′pG(2′p)3′p5′A that was produced in a control reaction by digestion of an *in vitro* spliced pre-tRNA substrate (Figure 9B, lane 3). Consistent with the assigned structure, treatment of either sample with snake venom phosphodiesterase (SVP) (which cleaves phosphodiester bonds even in the presence of a 2′-phosphate) quantitatively converted the labeled dinucleotides to pA. Furthermore, in a related approach, digestion with P1 nuclease liberated labeled pA if the spliced RNA was first treated with CIP to remove the 2′-phosphate at the splice junction (McCraith and Phizicky, 1990; data not shown). Thus by the criteria addressed here, the mechanism by which *HAC1*^{u} RNA exons become ligated by tRNA ligase is indistinguishable from that used during tRNA splicing.

Discussion

We have characterized the enzymatic mechanism by which Ire1p carries out the unique, spliceosome-independent splicing of *HAC1*^{u} mRNA and have defined a minimal substrate which is accurately cleaved by Ire1p(k+t). Though the mechanism of *HAC1*^{u} mRNA splicing resembles that of pre-tRNA splicing, our data also revealed differences between the two pathways. In particular, we have shown that Ire1p and tRNA endonuclease recognize fundamentally different structural features in their respective substrate RNAs. In some ways, this is not surprising given that these two nucleases lack any recognizable structural similarity. Indeed, the most similar protein to Ire1p is RNase L, a ribonuclease which non-specifically cleaves RNA in cells infected with double-stranded RNA viruses and for which no role in pre-mRNA processing is suspected (Bork and Sander, 1993; Hassel *et al*., 1993; Dong *et al*., 1994; Dong and Silverman, 1997; Zhou *et al*., 1997). Thus, though splicing of *HAC1*^{u} mRNA is unlike spliceosome-mediated pre-mRNA splicing, neither is it completely like pre-tRNA splicing. *HAC1*^{u} mRNA splicing thus defines a unique RNA processing event.

Our experiments have demonstrated that, mechanistically, splicing of *HAC1*^{u} mRNA resembles that of pre-tRNA splicing. In particular, as summarized in Figure 10, the chemistry of endonucleolytic cleavage by Ire1p leaves 2′,3′-cyclic phosphates, the two exons remain associated by base pairing after cleavage has occurred, and exon ligation by tRNA ligase follows the same chemical steps previously characterized for pre-tRNA splicing. This mechanism of processing is unprecedented for a messenger RNA.

By defining a minimal RNA element that is sufficient and required for cleavage by Ire1p(k+t), we have shown that the structural features which Ire1p recognizes in its substrate differ significantly from those which are recognized by tRNA endonuclease. Eukaryotic tRNA endonuclease, for example, primarily recognizes the folded tertiary structure of the pre-tRNA as well as local structures at the intron–exon boundaries and pays little heed to the nucleotide sequences at or near the splice sites (Mattoccia *et al*., 1988; Reyes and Abelson, 1988; Fabbri *et al*., 1998). Indeed, changing the length of the stem that separates the cleavage sites from the knee in the tRNA tertiary fold shifts the cleavage sites correspondingly (Reyes and Abelson, 1988). This indicates that eukaryotic tRNA endonuclease can use distance measurements from a substrate binding site to its active site to specify the cleavage sites on its substrate RNA. Recently, a small, doubly bulged stem containing both cleavage sites of pre-tRNA was shown to be a suitable substrate for tRNA endonuclease (Fabbri *et al*., 1998), indicating that, as for *HAC1*^{u} mRNA cleavage by Ire1p, local structural features in pre-tRNA can be sufficient to confer cleavage specificity. Archaeal tRNA endonuclease recognizes a symmetric, bulged stem structure, also with little regard for the

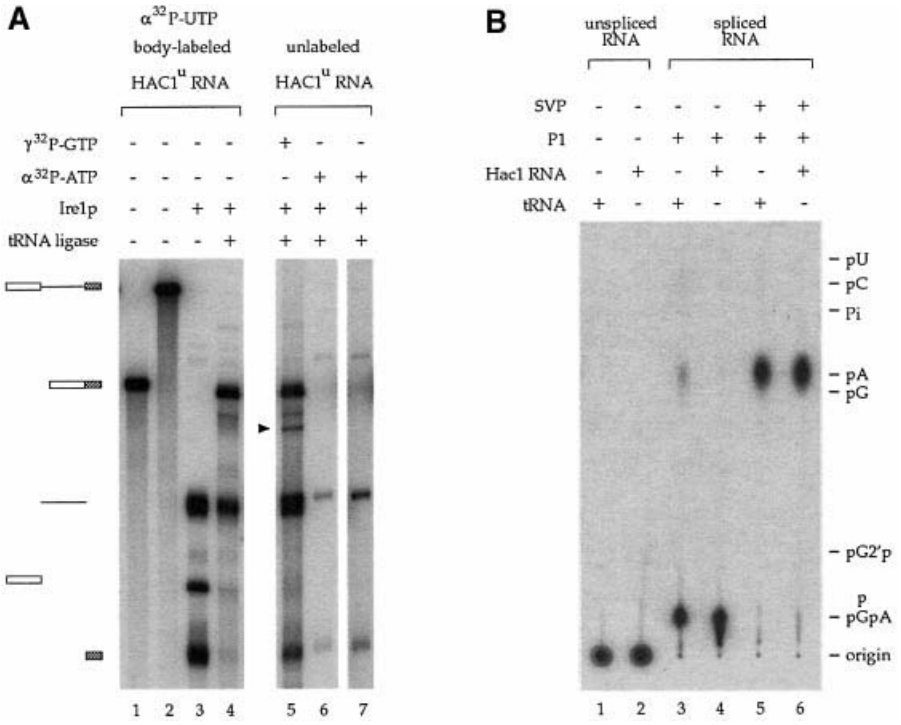

Fig. 9. The phosphate group at the splice junction derives from nucleotide triphosphate. (**A**) Unlabeled *HAC1*^{u} 600 RNA (1 pM), cleavage buffer and 0.5 µg Ire1p(k+t) were incubated at 30°C for 45 min. Then 0.3 µg purified tRNA ligase was added along with either 1 mM ATP, 65 µCi [γ-^{32}P]GTP (lane 5) or 200 µCi [α-^{32}P]ATP, 1 mM GTP (lanes 6 and 7), and the reaction incubated for another 30 min. Lanes 6 and 7 only differ in the length of time they were exposed to film. The remaining lanes carry markers derived from internally labeled *HAC1*^{u} RNA. *HAC1*^{u} 600 RNA was incubated in cleavage buffer with Ire1p(k+t) (lane 3), or Ire1p(k+t), tRNA ligase, ATP and GTP (lane 4). These two lanes provided markers for the Ire1p(k+t) cleavage reaction, and the products of the complete Ire1p(k+t)/tRNA ligase splicing reaction, respectively. Markers for uncleaved *HAC1*^{u} 600 RNA (lane 2) as well as *HAC1*^{i} 348 RNA corresponding to spliced *HAC1*^{u} 600 RNA (lane 1) are shown. Note that the labeled intron in lane 5 splits into a doublet; it is likely that these two forms correspond to a 5′-phosphorylated and a 5′-phosphorylated and also adenylated RNA, both known tRNA ligase reaction products. The nature of the band in lane 5 indicated by a triangle is unknown; one possibility is that it represents a circularized or concatenated intron. (**B**) *HAC1*^{u} 600 RNA spliced in the presence of [γ-^{32}P]GTP as in (A) was gel-purified from a 5% denaturing polyacrylamide gel, and subjected to nuclease P1 digestion (lane 4), followed by digestion with SVP (lane 6). Digestion products were chromatographed on PEI cellulose thin layer plates and visualized by autoradiography. Nuclease P1 digestion of *in vitro* spliced pre-tRNA^{Phe} (lane 3) provided a marker for the 5′pG(2′p)3′,5′pA splice junction dinucleotide (see Materials and methods) and SVP digestion provided a positive control for SVP digestion of spliced *HAC1*^{u} RNA. The position of other nucleotide markers on the thin layer plate is shown.

sequence surrounding the cleavage sites (Thompson and Daniels, 1990; Lykke-Andersen and Garrett, 1994, 1997; Kleman-Leyer *et al*., 1997). In contrast, we show that cleavage by Ire1p(k+t) requires a well defined 7-nucleotide loop that must be closed by a stem. Furthermore, unlike tRNA endonucleases, cleavage by Ire1p(k+t) is exquisitely sensitive to the particular nucleotide sequence flanking the cleavage site (Figures 2 and 3) (Sidrauski and Walter, 1997; Kawahara *et al*., 1998). With the exception of loop residue –2, changes at the other six loop positions can drastically reduce cleavage by Ire1p(k+t). The nucleotides at these sensitive positions may provide critical contacts for Ire1p and/or maintain specific structural arrangements within the loop necessary for Ire1p recognition. Thus, our data define a unique 'signature motif' for Ire1p substrates. This structural information will be invaluable for future studies whose aim is identification of other substrates for this unique RNA processing pathway in yeast and other organisms.

Though the primary sequence of the minisubstrate loops is important for Ire1p(k+t) recognition and cleavage, our data suggest that other sequences within *HAC1*^{u} mRNA significantly enhance recognition by Ire1p. In particular, *HAC1*^{u} RNA substrates carrying the entire intron plus flanking exon sequences were cleaved significantly faster than the minisubstrate stem–loop RNAs (Figure 7). Ire1p may have a higher affinity for these substrates relative to the minisubstrates, possibly because it interacts directly with additional regions of *HAC1*^{u} mRNA that fall outside the stem–loop structures. An alternative albeit not mutually exclusive explanation is that, as previously suggested, active Ire1p is a dimer or higher order oligomer that binds *HAC1*^{u} mRNA so that one monomer interacts with the 5′ splice site and the other interacts with the 3′ splice site (Sidrauski and Walter, 1997). Indeed Ire1p oligomerizes upon activation *in vivo* (Shamu and Walter, 1996), and addition of ADP to *in vitro* reactions stimulates Ire1p(k+t) dimerization/oligomerization (Niwa and Walter, unpublished results) and its endoribonuclease activity (Sidrauski and Walter, 1997). For this reason, all reactions described in this paper were performed under optimal ADP-stimulating conditions. A gain in affinity could result from cooperative binding of Ire1p to the two splice sites and thus lead to increased cleavage. Folding of the intron and/or base pairing interactions between the two exons may significantly contribute to cooperativity by positioning the two splice sites in an optimal orientation with respect to each other.

One of the unique consequences of the Ire1p/tRNA ligase-mediated splicing pathway is that the splice junction

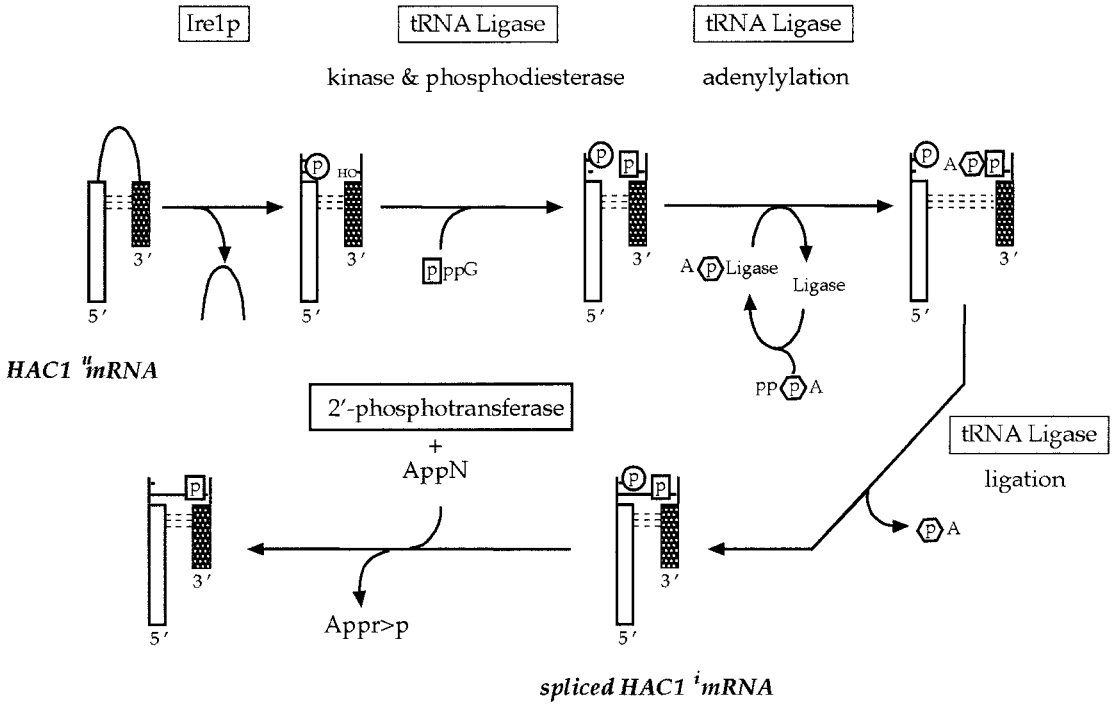

Fig. 10. Model of *HAC1*^{u} mRNA splicing. Ire1p initiates splicing by cleaving *HAC1*^{u} mRNA 3′ of the conserved G at position –1 in both splice site loops (Figures 1 and 3), releasing the intron and generating a 2′,3′-cyclic phosphate at the 3′ end of the 5′ exon and a free 5′-OH group at the 5′ end of the 3′ exon, respectively. The liberated exons remain base paired, thus holding the appropriate mRNA termini in spatial proximity. tRNA ligase acts upon the paired exons, phosphorylating the 5′ terminus of the 3′ exon with phosphate derived from the γ-position of GTP. This GTP-derived phosphate group ultimately links the two exons together in the spliced *HAC1*^{i} mRNA. The phosphodiesterase activity of tRNA ligase opens the 2′,3′-cyclic phosphate to the 2′ position. tRNA ligase next adenylates the 5′ terminus of the 3′ exon, forming a high energy A5′pp5′A phosphoanhydride bond and then, using the energy stored in this bond, joins the two exons. As is the case for pre-tRNA splicing, it is likely that tRNA ligase first adenylates itself and then transfers its AMP to the 3′ exon. Upon ligation of the exons, the AMP is released. The splice junction of the newly spliced *HAC1*^{i} mRNA carries a 2′-phosphate derived from the 5′ splice site. As for pre-tRNA splicing, perhaps NAD-dependent 2′-phosphotransferase transfers this phosphate to NAD to produce ADP-ribose 1′′-2′′ cyclic phosphate (Appr>p) and *HAC1*^{i} mRNA free of the splice junction 2′-phosphate.

of the product *HAC1*^{i} mRNA is initially tagged by a 2′-phosphate group. This tag marks the splice junction of all newly ligated *HAC1*^{i} mRNA molecules until it is presumably removed. In yeast, the product of an essential gene, a NAD-dependent 2′-phosphotransferase transfers 2′-phosphate groups from spliced tRNAs to NAD, producing ADP-ribose 1′′-2′′cyclic phosphate (McCraith and Phizicky, 1990; Culver *et al*., 1993, 1997). The same phosphotransferase may act upon newly ligated *HAC1*^{i} mRNA to remove its splice junction 2′-phosphate (Spinelli *et al*., 1997). It is not known whether the unique 2′-phosphate tag or the unique cyclic phosphate-containing metabolite that results from its removal have any physiological function in the cell (Culver *et al*., 1997). It is conceivable, however, that induction of the UPR, and the resulting splicing of *HAC1*^{u} mRNA might generate a spike of the unusual ADP-ribose 1′′-2′′ cyclic phosphate over the level normally produced as a consequence of pre-tRNA splicing. Thus it is tempting to speculate that cells might utilize such a signal, possibly in ways analogous to signals transmitted via other small molecules containing cyclic phosphate groups, and integrate it in as yet unknown ways into the cell's response to protein misfolding in the ER.

Materials and methods

Plasmid constructs and recombinant protein expression

The cytoplasmic portion of *S.cerevisiae* Ire1p containing its kinase and C-terminal tail domains, Ire1p(k+t), was expressed in and purified from *Escherichia coli* as previously described (Sidrauski and Walter, 1997). In this study, we used an expression vector which fuses a PreScission Protease (Pharmacia, Uppsala, Sweden) cleavage site between the Ire1p(k+t) and glutathione *S*-transferase (GST) domains of the recombinant polypeptide. In brief, *E.coli* strain DH5α transformed with plasmid pCF210 was grown in liquid culture at 37°C to an OD of 0.5. Expression of recombinant GST–Ire1p(k+t) was induced with isopropyl-β-D-galactopyranoside (IPTG) added to a final concentration of 0.1 mM. Cells were harvested and ruptured with a Microfluidizer (Microfluidics Co., Newton, MA). GST–Ire1p(k+t) was captured by batch binding to glutathione–Sepharose beads (Pharmacia, Uppsala, Sweden), and Ire1p(k+t) was liberated by digestion with PreScission Protease.

The gene encoding tRNA ligase was amplified from the *S.cerevisiae* genome by PCR and the sequence of the amplified gene was verified. The gene was cloned into the expression vector pGEX-6P-2 to create a GST–tRNA ligase fusion with a PreScission Protease cleavage site between GST and tRNA ligase. Expression of the recombinant protein from this plasmid (pSD103) was as for Ire1p(k+t) (see above). Harvested cells were ruptured by sonication and expressed GST–tRNA ligase was bound to glutathione–Sepharose beads. The beads were subsequently washed to remove non-recombinant protein and GST–tRNA ligase was eluted from the beads with 20 mM glutathione, pH 7.5. The eluted fusion protein was dialyzed to remove glutathione and cleaved with PreScission Protease to liberate tRNA ligase. In the final step, PreScission Protease and free GST were removed by incubating the cleaved material with glutathione–Sepharose beads, thus yielding pure tRNA ligase.

In vitro RNA transcription

In vitro transcriptions of *HAC1*^{u} 600, *HAC1*^{u} 508, *HAC*^{i} 348 [see Sidrauski and Walter (1997) for details of the plasmids encoding these RNAs] and pre-tRNA^{Phe} (from plasmid pUC12T7, a gift from C.Greer, University of California, Irvine) were carried out as follows. Reactions (20 μl) containing 1 mM each of ATP, CTP, GTP, 0.1 mM of UTP, 25 μCi of [α-^{32}P]UTP (3000 Ci/mM; Amersham, Arlington Heights, IL), 1 μg linearized plasmid DNA, 40 U RNasin (Promega, Madison,

WI), and 20 U T7 RNA polymerase (Boehringer Mannheim, Indianapolis, IN) were incubated at 37°C for 1.5 h. To generate unlabeled RNA, transcriptions were carried out in the presence of 1 mM UTP without [α-^{32}P]UTP.

Smaller RNAs were transcribed using single-stranded DNA oligonucleotides as templates to which the 18mer 5′TAATACGACTCACTATAG 'T7 promoter oligonucleotide' was annealed to create the double-stranded T7 RNA polymerase promoter (Milligan *et al*., 1987). The following oligonucleotides were used: hactng-10 (encoding wild-type 3′ stem–loop RNA): 5′TGAGGTCAAACCTGACTGCGCTTCGGACAGTACAAGCTTGACCTATAGTGAGTCGTATTA; hactng-32 (encoding 3′ stem–loop RNA with GC stem): 5′GAGCGGCGCGGCGCTTCGGACCGCGCCGCTATAGTGAGTCGTATTA; hactng-33 (encoding 3′ stem–loop RNA with GA stem): 5′GATCTTCTCTTCGCTTCGGACCTCTCCTCTATAGTGAGTCGTATTA; hactng-38 (encoding wild-type 5′ stem–loop RNA): 5′TGAGCCGGTCATCGTAATCACGGCTGGATTACGCCAACCGGCTATAGTGAGTCGTATTA, and hactng-39 (encoding 5′ stem–loop used in TLC analysis): 5′TGAGGGGGTCATCGTAATCACGGCTGGATTACGACAACCCCCTATAGTGAGTCGTATTA. Oligonucleotides containing the appropriate point mutations indicated in Figures 2B and 3 are modifications of hactng-10.

A solution containing 15 pM T7 promoter oligonucleotide and 0.25 pM template oligonucleotide was heated to 100°C for 3 min and immediately placed on ice. For the nearest neighbor analysis, RNA transcripts were internally labeled by incorporation of any one of three (A, C or G) [α-^{32}P]NTPs (3000 Ci/mM; Amersham Corporation, Arlington Heights, IL). In this case, all NTPs in the transcription reactions were at 1 mM, except the labeled NTP of which 300 μCi was added diluted with unlabeled NTP to bring the final concentration to 0.1 mM. To transcribe stem–loop RNAs internally labeled with [α-^{32}P]UTP (3000 Ci/mM; Amersham Corporation, Arlington Heights, IL), 1 mM each of ATP, CTP, GTP, 0.1 mM of UTP and 50 μCi [α-^{32}P]UTP were added to the reactions instead.

Except where noted, all transcribed RNAs were purified on denaturing polyacrylamide gels, excised from the gels and eluted from gel slices overnight at 4°C with 0.3 M NaOAc, pH 5.2, 10 mM $Mg(OAc)_2$/phenol/chloroform (1/0.5/0.5) followed by ethanol precipitation.

Ire1p(k+t) cleavage and splicing reactions

Ire1p(k+t) cleavage of *HAC1^u* 600 RNA, *HAC1^u* 508 RNA, and stem–loop RNAs was carried out in cleavage buffer [20 mM HEPES pH 7.6, 50 mM KOAc, 1 mM $Mg(OAc)_2$, 1 mM DTT, 2 mM ADP, 40 U RNasin (Promega, Madison, WI)] at 30°C. The amount of Ire1p(k+t) and RNA in the reactions varied and is given in the figure legends or specific methods for each experiment. For splicing reactions with internally radiolabeled *HAC1^u* 600 RNA, the RNA was first incubated with Ire1p(k+t) for 30 min at which point 1 mM ATP, 1 mM GTP and 0.3 μg tRNA ligase were added, and the reaction incubated for an additional 30 min at 30°C. Two different sets of splicing reactions were performed utilizing 1 pM unlabeled RNA each. In one, 65 μCi of [γ-^{32}P]GTP (5000 Ci/mM) (Amersham Corporation, Arlington Heights, IL) was added instead of GTP. In the other, 200 μCi [α-^{32}P]ATP (3000 Ci/mM) (Amersham Corporation, Arlington Heights, IL) was added instead of ATP. All reactions were terminated with 20 vol of stop buffer (50 mM NaOAc, pH 5.2, 1 mM EDTA, 0.1% SDS), extracted with phenol-chloroform, and ethanol-precipitated. Unless otherwise noted, reactions containing stem–loop RNAs and those containing the larger RNAs were analyzed on 15 and 5% denaturing polyacrylamide gels, respectively, and visualized by autoradiography of the gels.

Enzymatic modification of Ire1p(k+t) cleavage products

A 100 μl Ire1p(k+t) cleavage reaction containing cleavage buffer (see above), 10 000 c.p.m. wild-type 3′ stem–loop RNA, and 5 μg Ire1p(k+t) was incubated at 30°C for 2 h. The reaction was stopped with stop buffer (see above) and phenol-chloroform extracted. Two fifths of the reaction was removed and set aside. The remaining sample was ethanol precipitated and treated with 30 U CIP (New England Biolabs, MA) for 1.5 h at 37°C. The reaction was phenol–chloroform extracted, and one-third of the sample was set aside. The remaining sample was ethanol precipitated and treated with 30 U T4 polynucleotide kinase (New England Biolabs, MA) in the absence of ATP for 1.5 h at 37°C followed by phenol-chloroform extraction. Half of the sample was set aside, and the remaining sample was ethanol precipitated and treated with 30 U T4 polynucleotide kinase plus 2 mM ATP for 1.5 h at 37°C followed by phenol-chloroform extraction and ethanol precipitation. For analysis, all samples were ethanol precipitated, fractionated on a 15% denaturing polyacrylamide gel and visualized by autoradiography.

TLC analyses

Prior to digestion, the 5′ and 3′ stem–loop RNAs or the ligated products of the *HAC1^u* 600 and pre-tRNA^{Phe} splicing reactions were gel-purified and eluted overnight in water/phenol/chloroform (1/0.5/0.5) at 4°C. Eluted RNA was precipitated by extraction with N-butanol, washed with ethanol, and dried. P1 nuclease digests of 3′ and 5′ stem–loop RNAs were prepared by incubation of the RNA sample with 0.2 U P1 nuclease (Boehringer Mannheim, Indianapolis, IN) at 37°C for 30 min in a buffer that contained 0.5 μg tRNA and 20 mM NaOAc, pH 5.2. P1 digests of spliced *HAC1^u* 600 RNA as well as spliced pre-tRNA^{Phe} were the same but contained only 50 ng tRNA. For further digestion of the P1 nuclease products with SVP, the reaction mix was adjusted to 12.5 mM Tris pH 9.3 and 0.1 μg tRNA, and 0.025 U SVP (Worthington Biochemical Co., Freehold, NJ) were added. The reaction was incubated at 25°C for 40 min.

Spliced pre-tRNA^{Phe} and *HAC1^u* share the same splice junction sequence: G-junction-A (Valenzuela *et al*., 1978; Reyes and Abelson, 1987; Sidrauski and Walter, 1997; Kawahara *et al*., 1998). Because of this, spliced pre-tRNA^{Phe} was used to generate 5′pG(2′p)3′p5′A marker dinucleotide for the TLC analysis of the *HAC1^u* splice junction. To do so, pre-tRNA^{Phe} cleavage reactions were carried out in tRNA endonuclease buffer (Greer *et al*., 1987) for 30 min at 30°C. Unlabeled pre-tRNA^{Phe} (1 pM) was first incubated with tRNA endonuclease for 30 min as described (Greer *et al*., 1987), at which point 1 mM ATP, 0.3 μg tRNA ligase and 65 μCi of [γ-^{32}P]GTP (5000 Ci/mM) were added and the reaction incubated for an additional 20 min at 30°C. The resulting spliced tRNA^{Phe} was gel purified. To generate labeled 5′pG(2′p)3′p5′A, purified tRNA^{Phe} was digested with P1 nuclease as above. Further digestion with SVP as described above generated labeled pA as expected.

PEI cellulose thin layer plates (EM Science, Gibbstown, NJ) were developed with 1 M LiCl, and samples visualized by autoradiography. The radiolabeled markers 5′pN, 5′pN2′p, 5′pN3′p and pN2′3′(cyclic)p (where N = A, C, G or U) were prepared by phosphorylating N2′p, N3′p, and N2′3′(cyclic)p nucleotides (Sigma) in the presence of [γ-^{32}P]ATP and either wild-type T4 polynucleotide kinase (New England Biolabs, MA) or mutant T4 polynucleotide kinase (Boehringer Mannheim, Indianapolis, IN) lacking the 3′ phosphatase activity of the wild-type enzyme (Cameron and Uhlenbeck, 1977; Cameron *et al*., 1978).

Primer extension

The sequencing primers P1 (TGSP-3; 5′GAAGAAATCATTCAATTCAAATGAATTC) and P2 (TGSP-1; 5′GCTAGTGTTCTTGTTCACTG) were used to map the 5′ and 3′ Ire1p(k+t) cleavage sites in *HAC1^u* 508 RNA, respectively. Reactions contained 1 pM 5′ end-labeled primer, 10 ng Ire1p(k+t)-cleaved or uncleaved *HAC1^u* 508 RNA, 20 mM NaCl, 15 mM HEPES pH 7.6. Reactions were heated to 100°C for 3 min and slowly cooled to 40°C. Next, 0.1 mM dNTPs and 3 U AMV reverse transcriptase (Boehringer Mannheim, Indianapolis, IN) were added, and the reactions incubated at 40°C for 30 min. Sequencing ladders were generated in the same manner, except that reactions also contained 0.1 mM of either ddATP, ddCTP, ddGTP or ddTTP. Samples were analyzed on 10% denaturing polyacrylamide gels and visualized by autoradiography.

Non-denaturing gel electrophoresis

Ire1p(k+t) cleavage reactions were electrophoresed at 4°C through a 5% polyacrylamide gel in 1× TBE buffer. Bands were visualized by autoradiography, excised from the gel, and eluted overnight in 0.3 M NaOAc pH 5.2, 10 mM $Mg(OAc)_2$/phenol/chloroform (1/0.5/0.5) at 4°C. Eluted RNA was ethanol precipitated, resuspended in denaturing loading buffer (99% formamide, 1 mM Tris pH 7.8, 0.1 mM EDTA), boiled and loaded onto a 5% denaturing polyacrylamide gel. RNA was visualized by autoradiography.

Acknowledgements

We thank C.Greer (University of California, Irvine) for plasmid pUC12T7; C.Trotta and J.Abelson (Caltech) for purified tRNA endonuclease; and C.Patil (Walter laboratory, UCSF) for providing us with the secondary structure prediction of the HAC1^u mRNA intron used in Figure 1A. We also thank G.Culver for very helpful advice regarding TLC as well as L.Gonzalez, R.Gonzalez and J.Leber for their support throughout these studies. Special thanks go to M.Niwa, T.Powers, P.Peluso and A.Frankel for advice, discussions and comments on the manuscript. This work was supported by a UCSF Biomedical Science Research Career Enhancement Fellowship from the National Institute of

General Medical Science to T.N.G. and by grants from the National Institutes of Health to P.W. P.W. is an Investigator and C.S. is a Postdoctoral Associate of the Howard Hughes Medical Institute.

References

Abelson,J., Trotta,C.R. and Li,H. (1998) tRNA splicing. *J. Biol. Chem.*, **273**, 12685–12688.

Belford,H.G., Westaway,S.K., Abelson,J. and Greer,C.L. (1993) Multiple nucleotide cofactor use by yeast ligase in tRNA splicing. Evidence for independent ATP- and GTP-binding sites. *J. Biol. Chem.*, **268**, 2444–2450.

Bork,P. and Sander,C. (1993) A hybrid protein kinase-RNase in an interferon-induced pathway? *FEBS Lett.*, **334**, 149–152.

Cameron,V. and Uhlenbeck,O.C. (1977) 3′-Phosphatase activity in T4 polynucleotide kinase. *Biochemistry*, **16**, 5120–5126.

Cameron,V., Soltis,D. and Uhlenbeck,O.C. (1978) Polynucleotide kinase from a T4 mutant which lacks the 3′ phosphatase activity. *Nucleic Acids Res.*, **5**, 825–833.

Chapman,R.E. and Walter,P. (1997) Translational attenuation mediated by an mRNA intron. *Curr. Biol.*, **7**, 850–859.

Chapman,R., Sidrauski,C. and Walter,P. (1998) Intracellular signaling from the endoplasmic reticulum to the nucleus. *Annu. Rev. Cell Dev. Biol*, **14**, 459–485.

Cox,J.S. and Walter,P. (1996) A novel mechanism for regulating activity of a trancription factor that controls the unfolded protein response. *Cell*, **87**, 391–404.

Cox,J.S., Shamu,C.E. and Walter,P. (1993) Transcriptional induction of genes encoding endoplasmic reticulum resident proteins requires a transmembrane protein kinase. *Cell*, **73**, 1197–1206.

Culver,G.M., McCraith,S.M., Zillmann,M., Kierzek,R., Michaud,N., LaReau,R.D., Turner,D.H. and Phizicky,E.M. (1993) An NAD derivative produced during transfer RNA splicing: ADP-ribose 1′′-2′′ cyclic phosphate. *Science*, **261**, 206–208.

Culver,G.M., McCraith,S.M., Consaul,S.A., Stanford,D.R. and Phizicky,E.M. (1997) A 2′-phosphotransferase implicated in tRNA splicing is essential in *Saccharomyces cerevisiae*. *J. Biol. Chem.*, **272**, 13203–13210.

Di Nicola Negri,E., Fabbri,S., Bufardeci,E., Baldi,M.I., Gandini Attardi,D., Mattoccia,E. and Tocchini-Valentini,G.P. (1997) The eucaryal tRNA splicing endonuclease recognizes a tripartite set of RNA elements. *Cell*, **89**, 859–866.

Dong,B. and Silverman,R.H. (1997) A bipartite model of 2–5A-dependent RNase L. *J. Biol. Chem.*, **272**, 22236–22242.

Dong,B., Xu,L., Zhou,A., Hassel,B.A., Lee,X., Torrence,P.F. and Silverman,R.H. (1994) Intrinsic molecular activities of the interferon-induced 2–5A-dependent RNase. *J. Biol. Chem.*, **269**, 14153–14158.

Fabbri,S., Fruscoloni,P., Bufardeci,E., Di Nicola Negri,E., Baldi,M.I., Attardi,D.G., Mattoccia,E. and Tocchini-Valentini,G.P. (1998) Conservation of substrate recognition mechanisms by tRNA splicing endonucleases. *Science*, **280**, 284–286.

Gething,M.-J. and Sambrook,J. (1992) Protein folding in the cell. *Nature*, **355**, 33–45.

Greer,C.L., Peebles,C.L., Gegenheimer,P. and Abelson,J. (1983) Mechanism of action of a yeast RNA ligase in tRNA splicing. *Cell*, **32**, 537–546.

Greer,C.L., Soll,D. and Willis,I. (1987) Substrate recognition and identification of splice sites by the tRNA- splicing endonuclease and ligase from *Saccharomyces cerevisiae. Mol. Cell. Biol.*, **7**, 76–84.

Hammond,C. and Helenius,A. (1995) Quality control in the secretory pathway. *Curr. Opin. Cell Biol.*, **7**, 523–529.

Hassel,B.A., Zhou,A., Sotomayor,C., Maran,A. and Silverman,R.H. (1993) A dominant negative mutant of 2–5A-dependent RNase suppresses antiproliferative and antiviral effects of interferon. *EMBO J.*, **12**, 3297–3304.

Kawahara,T., Yanagi,H., Yura,T. and Mori,K. (1997) Endoplasmic reticulum stress-induced mRNA splicing permits synthesis of transcription factor Hac1p/Ern4p that activates the unfolded protein response. *Mol. Biol. Cell*, **8**, 1845–1862.

Kawahara,T., Yanagi,H., Yura,T. and Mori,K. (1998) Unconventional splicing of HAC1/ERN4 mRNA required for the unfolded protein response. Sequence-specific and non-sequential cleavage of the splice sites. *J. Biol. Chem.*, **273**, 1802–1807.

Kleman-Leyer,K., Armbruster,D.W. and Daniels,C.J. (1997) Properties of *H.volcanii* tRNA intron endonuclease reveal a relationship between the archaeal and eucaryal tRNA intron processing systems. *Cell*, **89**, 839–847.

Knapp,G., Ogden,R.C., Peebles,C.L. and Abelson,J. (1979) Splicing of yeast tRNA precursors: structure of the reaction intermediates. *Cell*, **18**, 37–45.

Kohno,K., Normington,K., Sambrook,J., Gething,M.J. and Mori,K. (1993) The promoter region of the yeast KAR2 (BiP) gene contains a regulatory domain that responds to the presence of unfolded proteins in the endoplasmic reticulum. *Mol. Cell. Biol.*, **13**, 877–890.

Kuznetsov,G. and Nigam,S.K. (1998) Folding of secretory and membrane proteins. *N. Engl. J. Med.*, **339**, 1688–1695.

Lykke-Andersen,J. and Garrett,R.A. (1994) Structural characteristics of the stable RNA introns of archaeal hyperthermophiles and their splicing junctions. *J. Mol. Biol.*, **243**, 846–855.

Lykke-Andersen,J. and Garrett,R.A. (1997) RNA–protein interactions of an archaeal homotetrameric splicing endoribonuclease with an exceptional evolutionary history. *EMBO J.*, **16**, 6290–6300.

Mattoccia,E., Baldi,I.M., Gandini-Attardi,D., Ciafre,S. and Tocchini-Valentini,G.P. (1988) Site selection by the tRNA splicing endonuclease of *Xenopus laevis*. *Cell*, **55**, 731–738.

McCraith,S.M. and Phizicky,E.M. (1990) A highly specific phosphatase from *Saccharomyces cerevisiae* implicated in tRNA splicing. *Mol. Cell. Biol*., **10**, 1049–1055.

Miao,F. and Abelson,J. (1993) Yeast tRNA-splicing endonuclease cleaves precursor tRNA in a random pathway. *J. Biol. Chem.*, **268**, 672–677.

Milligan,J.F., Groebe,D.R., Witherell,G.W. and Uhlenbeck,O.C. (1987) Oligoribonucleotide synthesis using T7 RNA polymerase and synthetic DNA templates. *Nucleic Acids Res.*, **15**, 8783–8798.

Moore,M.J., Query,C.C. and Sharp,P.A. (1993) Splicing of precursors to mRNAs by the spliceosome. In Gesteland,R.F. and Atkins,J.F. (eds), *The RNA World*. Cold Spring Harbor Laboratory Press, Cold Spring Harbor, NY, pp. 303–357.

Mori,K., Sant,A., Kohno,K., Normington,K., Gething,M.J. and Sambrook,J.F. (1992) A 22 bp *cis*-acting element is necessary and sufficient for the induction of the yeast KAR2 (BiP) gene by unfolded proteins. *EMBO J.*, **11**, 2583–2593.

Mori,K., Ma,W., Gething,M.J. and Sambrook,J. (1993) A transmembrane protein with a cdc2+/CDC28-related kinase activity is required for signaling from the ER to the nucleus. *Cell*, **74**, 743–756.

Mori,K., Kawahara,T., Yoshida,H., Yanagi,H. and Yura,T. (1996) Signalling from endoplasmic reticulum to nucleus: transcription factor with a basic-leucine zipper motif is required for the unfolded protein-response pathway. *Genes Cells*, **1**, 803–817.

Nikawa,J., Akiyoshi,M., Hirata,S. and Fukuda,T. (1996) *Saccharomyces cerevisiae* IRE2/HAC1 is involved in IRE1-mediated KAR2 expression. *Nucleic Acids Res.*, **24**, 4222–4226.

Peebles,C.L., Gegenheimer,P. and Abelson,J. (1983) Precise excision of intervening sequences from precursor tRNAs by a membrane-associated yeast endonuclease. *Cell*, **32**, 525–536.

Phizicky,E.M., Consaul,S.A., Nehrke,K.W. and Abelson,J. (1992) Yeast tRNA ligase mutants are nonviable and accumulate tRNA splicing intermediates. *J. Biol. Chem.*, **267**, 4577–4582.

Reyes,V.M. and Abelson,J. (1987) A synthetic substrate for tRNA splicing. *Anal. Biochem*., **166**, 90–106.

Reyes,V.M. and Abelson,J. (1988) Substrate recognition and splice site determination in yeast tRNA splicing. *Cell*, **55**, 719–730.

Shamu,C.E. and Walter,P. (1996) Oligomerization and phosphorylation of the Ire1p kinase during intracellular signaling from the endoplasmic reticulum to the nucleus. *EMBO J.*, **15**, 3028–3039.

Shamu,C.E., Cox,J.S. and Walter,P. (1994) The unfolded-protein-response pathway in yeast. *Trends Cell Biol.*, **4**, 56–60.

Sidrauski,C. and Walter,P. (1997) The transmembrane kinase Ire1p is a site-specific endonuclease that initiates mRNA splicing in the unfolded protein response. *Cell*, **90**, 1–20.

Sidrauski,C., Cox,J.S. and Walter,P. (1996) tRNA ligase is required for regulated mRNA splicing in the unfolded protein response. *Cell*, **87**, 405–413.

Sidrauski,C., Chapman,R. and Walter,P. (1998) The unfolded protein response: an intracellular signalling pathway with many surprising features. *Trends Cell Biol.*, **8**, 245–249.

Spinelli,S.L., Consaul,S.A. and Phizicky,E.M. (1997) A conditional lethal yeast phosphotransferase (tpt1) mutant accumulates tRNAs with a 2′-phosphate and an undermodified base at the splice junction. *RNA*, **3**, 1388–1400.

Thompson,L.D. and Daniels,C.J. (1990) Recognition of exon–intron boundaries by the *Halobacterium volcanii* tRNA intron endonuclease. *J. Biol. Chem.*, **265**, 18104–18111.

Tirasophon,W., Welihinda,A.A. and Kaufman,R.J. (1998) A stress response pathway from the endoplasmic reticulum to the nucleus

requires a novel bifunctional protein kinase/endoribonuclease (Ire1p) in mammalian cells. *Genes Dev.*, **12**, 1812–1824.

Trotta,C.R., Miao,F., Arn,E.A., Stevens,S.W., Ho,C.K., Rauhut,R. and Abelson,J.N. (1997) The yeast tRNA splicing endonuclease: a tetrameric enzyme with two active site subunits homologous to the archaeal tRNA endonucleases. *Cell*, **89**, 849–858.

Valenzuela,P., Venegas,A., Weinberg,F., Bishop,R. and Rutter,W.J. (1978) Structure of yeast phenylalanine-tRNA genes: an intervening DNA segment within the region coding for the tRNA. *Proc. Natl Acad. Sci. USA*, **75**, 190–194.

Wang,X.Z., Harding,H.P., Zhang,Y., Jolicoeur,E.M., Kuroda,M. and Ron,D. (1998) Cloning of mammalian Ire1 reveals diversity in the ER stress responses. *EMBO J.*, **17**, 5708–5717.

Welihinda,A.A. and Kaufman,R.J. (1996) The unfolded protein response pathway in *Saccharomyces cerevisiae.* Oligomerization and *trans*-autophosphorylation of Ire1p (Ern1p) are required for kinase activation. *J. Biol. Chem.*, **271**, 18181–18187.

Welihinda,A.A., Tirasophon,W., Green,S.R. and Kaufman,R.J. (1998) Protein serine/threonine phosphatase Ptc2p negatively regulates the unfolded-protein response by dephosphorylating Ire1p kinase. *Mol. Cell. Biol.*, **18**, 1967–1977.

Westaway,S.K. and Abelson,J. (1995) Splicing of tRNA Precursors. In Söll,D. and RajBhandary,U. (eds), *tRNA: Structure, Biosynthesis and Function*. ASM Press, Washington, DC, pp. 79–92.

Xu,Q., Teplow,D., Lee,T.D. and Abelson,J. (1990) Domain structure in yeast tRNA ligase. *Biochemistry*, **29**, 6132–6138.

Zhou,A. *et al*. (1997) Interferon action and apoptosis are defective in mice devoid of 2′,5′-oligoadenylate-dependent RNase L. *EMBO J.*, **16**, 6355–6363.

Received March 2, 1999; revised and accepted April 15, 1999